Conformational Analysis of 2-Substituted Alkylphosphoryl Compounds. 4. Substituent Effect on the Nature of the Hydrogen Bonding in (2-Hydroxyalkyl)phosphoryl Systems

Daniel G. Genov, Roman A. Kresinski, and John C. Tebby*

Division of Chemistry, School of Sciences, Staffordshire University, Stoke-on-Trent ST4 2DE, U.K.

Received November 5, 1997

The extent to which solid state conformational and hydrogen bonding preferences of five (2-hydroxyalkyl)phosphoryl compounds **2a**−**e** [$R^1{}_2P(O)CH_2CH(OH)R^2$; **2a**, R^1 = MeO, R^2 = Ph; **2b**, $R^1 = R^2$ = Ph; **2c**, R^1 = Ph, R^2 = Bu^t; **2d**, R^1 = Me, R^2 = Ph; **2e**, R^1 = Me, R^2 = Bu^t] change upon dissolution has been investigated using X-ray crystallography, IR, and NMR spectroscopy. Intermolecular hydrogen bonding involving inversion-center-related cyclic dimers is shown to be a common solid state arrangement, with relatively small structural changes producing infinite chains. Intramolecular hydrogen bonded monomers are uncommon. Conflicting X-ray and IR evidence on the equivalence of hydrogen bonding in the dimeric structure of **2b** in the solid state is discussed. The changes in hydrogen bonding occurring upon dissolution have been studied and evidence presented that an equilibrium between dimers and monomers is usually set up, which can become extensively shifted to a predominance of intramolecular hydrogen bonded monomers when bulky groups (R^1 and R^2) are present. Conformational preferences are determined mainly by steric factors (the size of R^2) and little influenced by changes in the nature of the hydrogen bonding or donation of electrons from the hydroxyl oxygen to vacant orbitals of the phosphorus atom. The extent of distortion from perfectly staggered geometries, upon which most conformational analyses are based, has been estimated to be 4 to 12° for two of the compounds. Ab initio and molecular mechanics solvation studies have been used to explain NMR chemical shift trends of the α-methylene protons and the phosphorus nucleus. Large chemical shift differences between the α-methylene protons of diphenylphosphine oxides **2b** and **2c** in acetone-d_6 are attributed to the specific orientation of acetone-d_6 molecules toward one of the protons in the major conformer.

Introduction

(2-Hydroxyalkyl)phosphine oxides and phosphonates are intermediates in the Horner−Wittig and Horner−Wadsword−Emmons reactions.[1] However, there have been few studies on the solid state and solution structures of such compounds. In NMR studies on the conformational preferences of (2-hydroxyalkyl)phosphonates in solution, intramolecular hydrogen bonding was invoked to explain the preponderance of the conformer with a gauche orientation between the phosphoryl and the hydroxyl group and anti orientation between the former group and the alkyl group (*ga*).[2] The crystal structures of (2-hydroxyalkyl)phosphine oxides **1a**−**c** have been elucidated solely to assign the configurations of the chiral centers.[3] In these studies both intermolecular (**1a,b**)[3a,c] and intramolecular (**1c**)[3b] hydrogen bonding in the solid state have been observed. The solution structures of phosphine oxides **1a**−**c** have not been determined. Studies on the solution and solid-state structures of diethyl (2-hydroxyalkyl)phosphonates (**1d**−**i**) have shown that while the compounds adopt the same conformer (*ga*) in both phases, the P═O---HO hydrogen bonding changes from intermolecular in the solid state to intramolecular in solution.[4] The conformational preference has been attributed[4a,b] to the presence of stabilizing n(p)→d donation of the nonbonding electrons of the hydroxyl oxygen to the vacant d orbitals of phosphorus, the effect operating in addition to and independently of any intramolecular hydrogen bonding that may occur.

$MePhP(O)C(Me)_2CH(OH)Me$

(2*RS*,P*SR*)

1a

$R_2{}^1P(O)CHR^3CH(OH)R^2$

1b: *(1RS,2RS,2'RS)* R^1 = Ph, R^2 = Me, R^3 = CH(Me)NHCOPh
c: *(1RS,2SR)* R^1 = Ph, R^2 = Ph, R^3 = Me
d: *(1RS,2RS)* R^1 = EtO, R^2 = Pr^i, R^3 = 1-cyclohexenyl
e: *(1RS,2RS)* R^1 = EtO, R^2 = CH_2Ph, R^3 = 1-cyclohexenyl
f: *(1RS,2RS)* R^1 = EtO, R^2 = Ph, R^3 = 1-cyclohexenyl
g: *(1RS,2RS)* R^1 = EtO, R^2 = p-nitrophenyl, R^3 = vinyl
h: *(1RS,2SR)* R^1 = EtO, R^2 = p-nitrophenyl, R^3 = vinyl
i: *(1RS,2RS)* R^1 = EtO, R^2 = Ph, R^3 = Ph

(1) (a) Clayden, J.; Warren, S. *Angew. Chem., Int. Ed. Engl.* **1996**, *35*, 241−270. (b) Lawrence, N. J. *Prepr. Alkenes* **1996**, 19−58. (c) Maryanoff, B. E.; Reetz, A. B. *Chem. Rev.* **1989**, *89*, 863−927.

(2) (a) Belciug, M.-P.; Modro, A. M.; Modro, T. A.; Wessels, P. L. *J. Phys. Org. Chem.* **1992**, *5*, 787−794. (b) Belciug, M.-P.; Modro, T. A.; Wessels, P. L. *J. Phys. Org. Chem.* **1993**, *6*, 523−530. (c) Genov, D. G.; Tebby, J. C. *J. Org. Chem.* **1996**, *61*, 2454−2459.

(3) (a) Allen, F.; Kennard, O.; Nassimbeni, L.; Shepherd, R.; Warren, S. *J. Chem. Soc., Perkin Trans. 2* **1974**, 1530−1536. (b) Buss, A. D.; Cruse, W. B., Kennard, O.; Warren, S. *J. Chem. Soc., Perkin Trans. 1* **1984**, 243−247. (c) Cavalla, D.; Cruse, W. B.; Warren, S. *J. Chem. Soc., Perkin Trans. 1* **1987**, 1883−1898.

(4) (a) Gerber, K. P.; Roos, H. M.; Modro, T. A. *J. Mol. Struct.* **1993**, *296*, 85−93. (b) Müller, E. L.; Roos, H. M.; Modro, T. A. *J. Phys. Org. Chem.* **1993**, *6*, 64−70. (c) Angelova, C.; Macicek, J.; Vassilev, N. G.; Momchilova, S.; Petrova, J. *J. Cryst. Spectrosc.* **1992**, *22(3)*, 253−258.

S0022-3263(97)02036-7 CCC: $15.00
Published on Web 03/25/1998

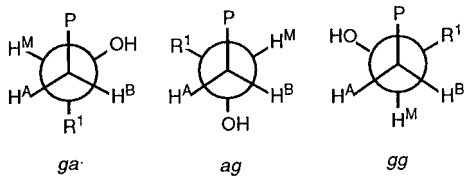

Figure 1. Three staggered conformers arising by rotation about the C1−C2 bond of **2** [P = $R^1{}_2P(O)$].

The above examples demonstrate the diversity of the hydrogen bonding in (2-hydroxyalkyl)phosphoryl compounds. However, no attention has been paid to the effect of substituents on the phosphorus atom or the alkyl chain on the nature of the hydrogen bonding. Clearly more investigations are necessary in order to estimate the contribution of the hydrogen bonding in determining the conformational preferences. In the present study X-ray, IR, NMR, and molecular modeling have been used to investigate hydrogen bonding and conformational equilibria (Figure 1) of phosphonate **2a** and phosphine oxides **2b**−**e** in both the solid and liquid states.

Results and Discussion

Synthesis. (2-Hydroxy-2-phenylethyl)diphenylphosphine oxide (**2b**) and (2-hydroxy-3,3-dimethylbutyl)diphenylphosphine oxide (**2c**) were prepared from diphenylmethylphosphine oxide and the corresponding aldehyde in THF (eq 1).[5]

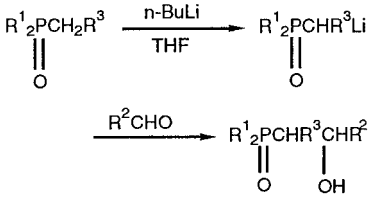

2a: R^1 = MeO, R^2 = Ph, R^3 = H
b: R^1 = Ph, R^2 = Ph, R^3 = H
c: R^1 = Ph, R^2 = Bu^t, R^3 = H
f: R^1 = Ph, R^2 = Pr^n, R^3 = H **(1)**

Dimethyl (2-hydroxy-2-phenylethyl)phosphonate (**2a**) was synthesized in a similar manner from dimethyl methylphosphonate and benzaldehyde.[2c] (2-Hydroxy-2-phenylethyl)dimethylphosphine oxide (**2d**) and (2-hydroxy-3,3-dimethylbutyl)dimethylphosphine oxide (**2e**) were obtained by the reaction of diethyl phosphite (diethyl hydrogen phosphonate) with 3 equiv of methylmagnesium chloride in THF, followed by the alkylation of the intermediate chloromagnesium dimethyl phosphinite with an excess of appropriate epoxide (eq 2).[6]

Hydrogen Bonding and Conformational Preferences in the Solid State. Single-crystal X-ray diffraction studies of compounds **2a**−**e** revealed that these materials adopt a variety of hydrogen bonding preferences in the solid state. Table 1 contains details relating to data collection and structure solution and refinement, Table 2 contains selected interatomic distances and angles for the structure of **2a**. As is normally found for this class of compounds,[3,4] conformer *ga* is adopted by **2a**−**e** in the solid state. The hydrogen bonding is

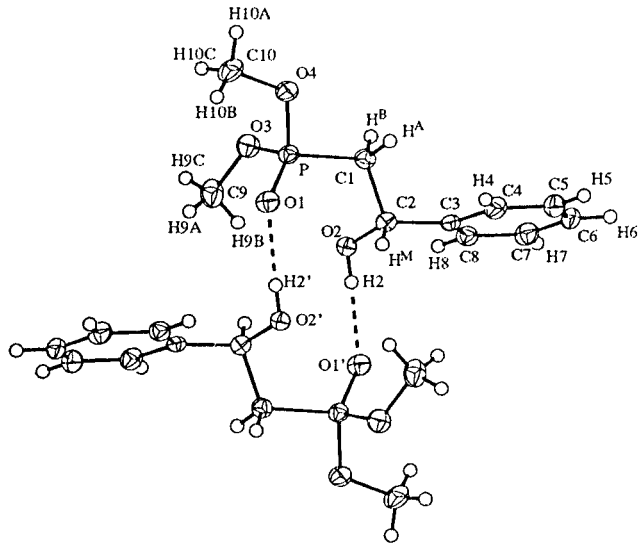

Figure 2. Crystal structure of **2a** (′ = 1 − x, −y, 1 − z).

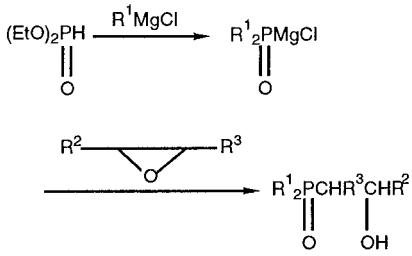

2d: R^1 = Me, R^2 = Ph, R^3 = H
e: R^1 = Me, R^2 = Bu^t, R^3 = H **(2)**

determined by the O−P−C−C torsion angle. Angles of 37−52° allow the P−O and O−H vectors to become parallel, resulting in the formation of dimers around crystallographic inversion centers, as is the case in **2a**, **2b**, and **2e**. Thus the structure of **2a** consists of dimers of molecules of opposite chirality (Figure 2); the intermolecular O1---O2′ (′ = 1 − x, −y, 1 − z) distance is 2.735(2) Å which is clearly indicative of hydrogen bonding, especially as the C2′−O2′---O1 angle is 112.2(2)°, apparently lending the oxygen a favorable tetrahedral hybridization.

The structure of **2b** contains two crystallographically independent molecules, each of which binds to its own symmetry equivalent (Figure 3) resulting in independent dimers. One of these dimers (that containing P51) is more distorted than the other. There is compensation for this through the formation of a stronger hydrogen bond, as shown by an O51---O52″ (″ = 1 − x, 1 − y, 2 − z) separation of 2.667(4) Å and C52″−O52″---O51 angle of 105.3(4)°, compared with values of 2.694(4) Å for O1---O2′ and 116.5(4)° for C2′−O2′---O1. It is possible that the distortions in **2b** arise from general packing forces. The apparent difference between the hydrogen bond lengths observed in the two dimers deserves further comment. The fact that only a single OH band is observed in the solid-state IR spectra of **2b** (see later) led us to query whether the two hydrogen bonds are indeed of significantly different lengths. However, the possibility of a higher symmetry space group making the two equivalent can be ruled out due to qualitative differences in the environments of the two dimers. Another possibility is that the stated error limits associ-

(5) Buss, A. D.; Warren, S. *J. Chem. Soc., Perkin Trans. 1* **1985**, 2307−2325.
(6) Hays, H. R. *J. Org. Chem.* **1968**, *33*, 3690−3694.

Table 1. Crystallographic Data for 2a−e

	2a	2b	2c	2d	2e
formula	$C_{10}H_{15}O_4P$	$C_{20}H_{16}O_2P$	$C_{18}H_{23}O_2P$	$C_{10}H_{15}O_2P$	$C_8H_{19}O_2P$
mol wt	230.19	322.32	302.33	198.19	178.2
color	none	none	none	none	none
size [mm^3]	0.22 × 0.32 × 0.26	0.26 × 0.18 × 0.20	0.32 × 0.28 × 0.05	0.22 × 0.18 × 0.24	0.24 × 0.10 × 0.08
mounting method	oil	cyanoacrylate	grease	grease	grease
temperature [K]	140	293	150	150	150
crystal system	monoclinic	anorthic	monoclinic	monoclinic	orthorhombic
space group	*C*2/*c*	*P*$\bar{1}$	*Pn*	$P2_1/c$	*Pbca*
Z	8	4	2	4	8
a [Å]	14.575(3)	10.195(3)	9.4461(6)	6.9760(12)	12.3504(8)
b [Å]	14.485(2)	13.268(3)	9.4431(9)	13.402(2)	9.9112(5)
c [Å]	10.809(2)	13.750(2)	10.2038(9)	11.531(2)	17.662(2)
α [deg]	90	93.502(9)	90	90	90
β [deg]	91.768(8)	101.415(11)	110.143(7)	96.091(14)	90
γ [deg]	90	109.238(10)	90	90	90
V [Å^3]	2280.9(7)	1705.3(7)	854.51(12)	1072.0(3)	2161.9(3)
d(c) [g cm^{-3}]	1.341	1.255	1.175	1.228	1.095
μ [mm^{-1}]	0.233	0.168	0.163	0.224	0.214
2*θ* [deg]	3.96−50	4.16−50	4.32−50	4.68−50	5.68−50
range	$-15 \le h \le 14$	$-1 \le h \le 11$	$-7 \le h \le 11$	$-7 \le h \le 7$	$-14 \le h \le 14$
	$-15 \le k \le 15$	$-15 \le k \le 15$	$-10 \le k \le 11$	$-11 \le k \le 14$	$-11 \le k \le 8$
	$-8 \le l \le 11$	$-15 \le l \le 11$	$-11 \le l \le 10$	$-13 \le l \le 12$	$-20 \le l \le 19$
reflns measd	4631	7086	3586	4246	7941
indep reflns	1704	4609	2008	1627	1751
obsd [$I > 2\sigma(I)$]	1476	2120	1817	1093	1190
parameters	142	419	197	124	109
R [$I > 2\sigma(I)$]	0.0465	0.0591	0.0463	0.0530	0.0316
*wR*2 (all data)	0.1168	0.1443	0.1195	0.1261	0.0647
GOF (all data)	1.048	0.783	1.117	0.934	0.850
peak [e/Å^3]	0.380	0.282	0.474	0.595	0.187
hole [e/Å^3]	0.305	0.228	0.275	0.319	0.199

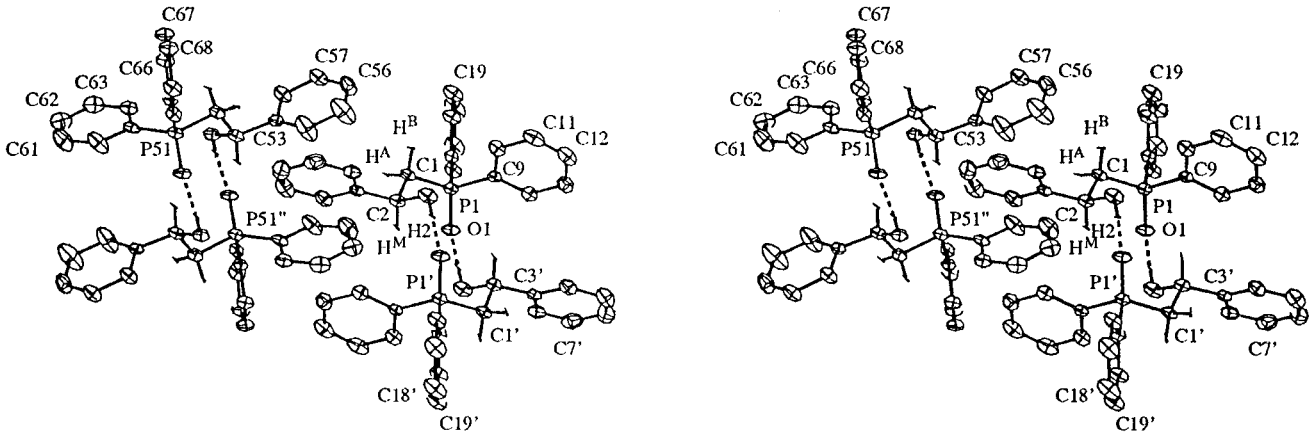

Figure 3. Stereoview of the crystal structure of **2b**. Phenyl hydrogens have been omitted for clarity, and all rings are numbered according to the same convention (′ = 1 − x, −y, 1 = z; ″ = 1 − x, 1 − y, 2 − z).

Table 2. Essential Bond Distances (Å) and Angles (deg) in 2a

P−O1	1.476(2)	P−O3	1.572(2)
P−O4	1.576(2)	P−C1	1.791(2)
O2−C2	1.419(2)	C1−C2	1.530(3)
C2−C3	1.518(3)		
O1−P−O3	113.29(8)	O1−P−O4	114.36(9)
O3−P−O4	101.72(9)	O1−P−C1	115.12(10)
O3−P−C1	109.76(10)	O4−P−C1	101.19(9)
C2−C1−P	113.3(2)	O2−C2−C3	113.2(2)
O2−C2−C1	106.2(2)	C3−C2−C1	110.7(2)
P−C1−C2−O2			55.8(2)
P−C1−C2−C3			179.1(1)
O1−P−C1−C2			−37.0(2)
H^A−C1−C2−H^M			60.1(2)
H^B−C1−C2−H^M			177.3(2)

ated with the two lengths may be underestimated, but the degree to which they should be revised upward is not clear. Certainly no strong correlations between these groups and/or others are evident but, should any exist, the fact that the data for **2b** were collected at a higher temperature (Table 1) may mean that error limits for this structure may be underestimated relative to **2a**, **2c**−**e**.

Phosphine oxide **2c** is unique among **2a**−**e** in that it is intramolecularly hydrogen bonded in the solid state (Figure 4). The O1−P−C1−C2 torsion angle brings O1 and O2 within a separation of 2.838(4) Å which is longer than those for **2a**, **2b**, and **2d** and represents a weaker hydrogen bond. The P−O1---O2 angle in **2c** of only 87.2(3)° implies either a nonlinear hydrogen bond or a rather uncommon and probably strained geometry at O1. As for **2a**−**e**, the structure refinement utilized a tetrahedral angle at O2 but, since the hydroxyl hydrogen was not precisely locateable in the final Fourier synthesis for **2c**, no further conclusion can be drawn.

In the solid state, **2d** is intermolecularly hydrogen bonded with symmetry-equivalent molecules, resulting

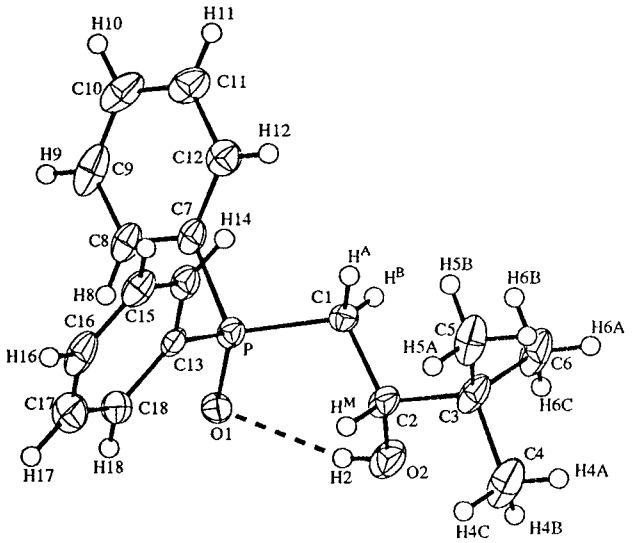

Figure 4. Crystal structure of **2c**.

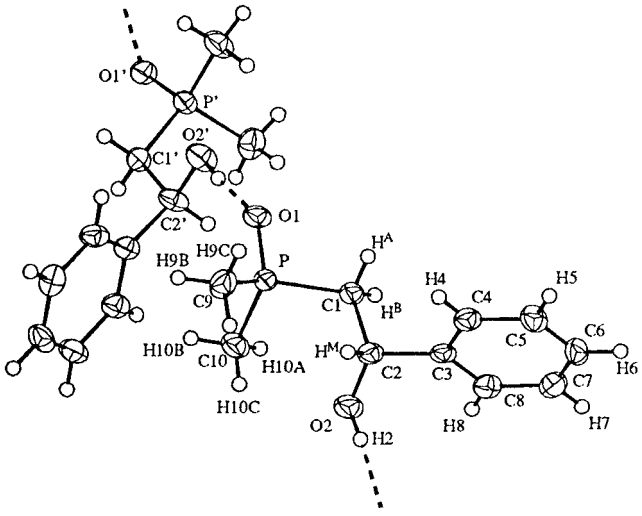

Figure 5. Crystal structure of **2d** (′ = 1 − x, y − 0.5, 1.5 − z).

(in the centrosymmetric space group) in two infinite chains of opposite chirality (Figure 5) extending along the crystal *b*-axis. The intermolecular O1---O2′ {′ = 1 − x, y − $^1/_2$, $1^1/_2$ − z) separation is 2.669(3) Å.

Phosphine oxide **2e**, like **2a** and **2b**, adopts a structure consisting dimers of opposite chirality (Figure 6). The tertiary butyl moiety appears almost perfectly staggered with respect to the carbon backbone, the C1−C2−C3−C4 torsion angle being 180.0(2)°. The hydrogen bonded O1---O2′ (′ = 2 − x, −y, −z) distance is 2.672(2) Å.

A comparison of the structures of **2a**−**e** with those of compounds **1a**−**i**[3,4] shows that **1b** is exceptional[3c] in that it is the only compound to adopt conformer *gg*, possibly as a result of the packing requirements of the large R^3 group. In comparison polymeric (2-hydroxypentyl)diphenylphosphine oxide (**2f**)[7] has its hydroxyl group disordered over two sites, the major conformer being *ag*, the minor conformer being *gg*. Both hydroxyl positions are hydrogen bonded to the phosphoryl group, conformer *ag* resulting in an intermolecular interoxygen separation of 2.761(7) Å, and conformer *gg*, 2.743(7) Å. Compounds

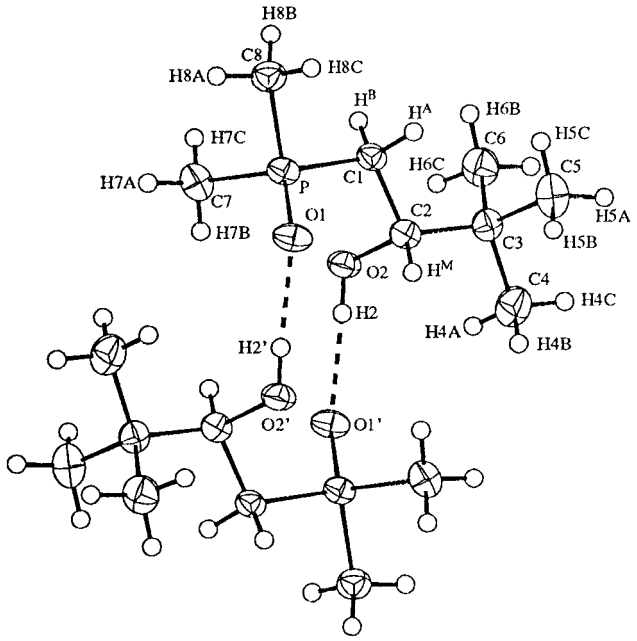

Figure 6. Crystal structure of **2e** (′ = 2 − x, −y, −z).

2a, **2b**, and **2e** join **1b** and **1e**−**i** in adopting what is emerging as a common solid state hydrogen bonding arrangement in acyclic (2-hydroxyalkyl)phosphoryl compounds, namely that of inversion-center-related dimers. The variation in intermolecular hydrogen bonded distances in **2a**, **2b**, and **2e** falls within the 2.649(8)−2.803(3) Å range displayed by **1b** and **1e**−**i**. Of these distances in **2**, that of **2a** is considerably the longer, despite the combined substituents of **2a** being, debatably, less bulky than those in **2b** and **2e**. This dissimilarity of **2a** is attributable to the electron-withdrawing effect of the methoxy groups reducing the basicity of the phosphoryl oxygen.

The structures of **2b** and **2c** may be contrasted with that of **1c**[3b] which differs from **2b** only by the replacement of H^A (and $H50^A$) by a methyl group. Phosphine oxide **1c**, like **2c**, adopts the rare intramolecular hydrogen bonding mode. However, it has an O1---O2 separation of only 2.738(4) Å, implying a hydrogen bond of comparable strength to **2a**, and much stronger than **2c**. The adoption of a radically different form of solid-state hydrogen bonding when H is replaced by Me for $R^1 = R^2$ = Ph implies that **2b** is more sterically congested than **2a** and **2e** and is close to the point at which general steric crowding disfavors dimer formation despite the hydrogen bonding interoxygen distances being fairly close. The reasons for the apparent weakness of the hydrogen bond in **2c** as compared to that in **1c** are, likewise, obscure.

The intermolecular chain formation adopted by **2d** resembles that of **1a**, **1d**, and **2f**. Of these, **2d** has the shortest hydrogen bonding interoxygen distance of 2.669(3) Å compared with 2.715(7) Å for **1a**,[8] 2.740(8) Å for **1d**, 2.743(7) Å and 2.761(7) Å for **2f**. Once again, an electronic effect may be invoked to account for this difference, **2d** bearing two methyl substituents on the phosphoryl group instead of the less "electron-donating" substituents borne by **1a**, **1d**, and **2f**.

One feature which all of **1** and **2**, except **1b** and **2f**, share, however, is the adoption of conformer *ga* in the

(7) Genov, D. G.; Kresinski, R. A.; Tebby, J. C. *Heteroatom Chem.* **1996**, *7*, 375−382.

(8) The unfeasibly large error limits reported[3a] for the early structural determination of **1a** were revised downward.

solid state. This has been attributed[4a,b] to an intramolecular interaction between the lone pairs of the hydroxyl oxygen and vacant d-orbitals of phosphorus, an effect which operates in addition to any intramolecular hydrogen bonding. Several observations indicate that this effect is not a significant one. First, **2f** contains probable disorder which results in an unequal distribution of molecules between conformers *ag* and *gg*. Conformer *ag* predominates, which suggests any O→P donation is not strong. Second, a significant interaction between phosphorus and hydroxyl oxygen should increase the R¹—P═O angle on the side of the C—P═O plane in which the hydroxyl group falls. An analysis of three of those structures,[4,9] which prompted the hypothesis of intramolecular O→P donation, reveals a spread of only 114.3−117.2° for the nonphosphoryl intersubstituent angles, indicating little perturbance of this environment by the proximal oxygen atom. Last, if an O→P interaction is strong, the C−O---P angle must be consistent with the hybridization of the oxygen as inferred from postulated hydrogen bonding interactions. In all compounds **1** and **2**, the hydrogen bonding geometry is consistent[10] with sp^3-hybridization at the hydroxyl oxygen (which would in any case direct oxygen lone pairs away from the P atom). The intramolecular C−O(hydroxyl)−P geometry in **2** varies from 48.3° (gauche) in **2f** to 67.3° in **2a** and in **1d**−**f**, from 68.0° to 70.0°, implying that any conventionally hybridized hydroxyl oxygen would interact only weakly with phosphorus.

Comparison of Hydrogen Bonding and Conformational Preferences in the Solid State with those in $DCCl_3$ and Tetrachloromethane Solutions. A. Studies Based on IR Spectroscopy. IR spectroscopic studies of the OH stretching region of compounds **2a**−**e** were carried out in order to compare the nature of the hydrogen bonding in the solid state and in $DCCl_3$ and tetrachloromethane solutions and to investigate its dependence on substituents R¹ and R² (Table 3).

The type of the hydrogen bonding of phosphonate **2a** (R¹ = MeO; R² = Ph) is strongly dependent on the solvent and the solution concentration. The cyclic dimers, established by X-ray diffraction studies, produce a single OH absorption band at 3309 cm^{-1} in the solid state. In concentrated tetrachloromethane solutions these dimeric structures are predominant and are in equilibrium with a small proportion of intramolecular hydrogen bonded monomers. Upon dilution the equilibrium shifts toward intramolecular hydrogen bonded monomers. Thus for a 2.2 mol % solution, the band arising from intermolecular hydrogen bonded dimers (as in the crystal) has a maximum at 3351 cm^{-1}. Lattice forces may be responsible for the lower wavenumber (3309 cm^{-1}) in the solid state since a similar difference was not observed for liquid phosphonates.[11] Dissymmetry at the higher frequency side of the band was observed, indicating the presence of a small quantity of intramolecular hydrogen bonded monomers in solution. These deductions were supported by the average molecular weight of phosphonate **2a**, determined by boiling point elevation in 2.2 mol % tetrachloromethane solution, which was 424 compared with monomer molecular mass 230. In less concentrated solutions this band loses intensity, and a higher frequency band due to intramolecular hydrogen bonded monomers develops at about 3450 cm^{-1}, its intensity increasing upon dilution. From 0.1 mol % to 1×10^{-3} mol % only this band is observed. In $DCCl_3$ the intramolecular hydrogen bonded monomers (about 3440 cm^{-1}) are the major species even in highly concentrated solutions. However small quantities of intermolecular hydrogen bonded dimers are present in these solutions as shown by a deflection at the lower frequency side of the band, which decreases upon dilution. The presence of dimers (broad band at 3399 cm^{-1}) is only significant in 4.3 mol % solution. Species with free OH groups (3604 cm^{-1}) are present in all solutions.

Table 3. Hydroxyl Stretching Wavenumbers (cm^{-1}) of Compounds 2 in the Solid State, in Tetrachloromethane and Chloroform-*d* Solutions

compd	solvent	C (mol %)	bonded OH	free OH
2a		solid[a]	3309	*b*
	CCl_4	2.2	3351	3614
		0.9	3349, 3450 (sh)	3615
		0.5	3352, 3446 (d)	3615
		0.2	3361 (sh), 3452	3617
		0.1	3457	3617
		3×10^{-3}	3457	*b*
		1×10^{-3}	3455	*b*
	$DCCl_3$	4.3	3399	3604
		2.2	3434	3604
		1.5	3441	3604
		1.1	3444	3604
		0.2	3447	3604
2b		solid	3197	*b*
	$DCCl_3$	4.3	3380	3602
		2.2	3390	3605
		1.1	3390	3606
		0.2	3393	3608
	CCl_4	3×10^{-3}	3397	*b*
2c		solid	3438	*b*
	$DCCl_3$	2.2	3414	3621
		1.1	3412	3620
		0.2	3410	3610
	CCl_4	3×10^{-3}	3417	*b*
2d		solid	3185	*b*
	$DCCl_3$	4.3	3267	3604
		2.2	3291	3607
		1.1	3304	3610
		0.9	3319	3607
		0.7	3341	3608
		0.5	3348	3607
		0.4	3363	3610
		0.2	3369	3608
	CCl_4	3×10^{-3}	3379	*b*
2e		solid	3217	*b*
	$DCCl_3$	4.3	3339	3626
		2.2	3359	3628
		1.1	3372	3628
		0.4	3389	3625
		0.2	3398	3628
	CCl_4	3×10^{-3}	3407	*b*

[a] KBr dispersion. [b] A band was not observed in this region.

The IR studies of phosphine oxides **2b**−**e** were carried out mainly on $DCCl_3$ solutions due to low solubility in tetrachloromethane. For diphenylphosphine oxide **2b** (R² = Ph) the nature of the hydrogen bonding in $DCCl_3$ solution (3390 cm^{-1}) is different from the dimeric structure in the solid state (3197 cm^{-1}). The band at 3390 cm^{-1} does not change appreciably upon dilution, indicating that in $DCCl_3$ solutions phosphine oxide **2b** forms intramolecular hydrogen bonded monomers. The spectra in $DCCl_3$ also exhibit a weak band at about 3606 cm^{-1}

(9) Allen, F. H.; Kennard, O. *Chem. Des. Automat. News* **1993**, *8(1)*, 1 and 31−37.

(10) In **2c**, the O1−H2−O2 and C2−O2−P planes differ by only 9° albeit that the former was determined using a fixed tetrahedral angle at O2.

(11) Genov, D. G.; Tebby, J. C. *Phosphorus, Sulfur, Silicon* **1996**, *114*, 91−98.

due to free OH groups. The appearance of only one single narrow band at 3197 cm^{-1} in the solid state was investigated further since X-ray crystallography had identified two different hydrogen bonded dimers. The IR band remained narrow for both KBr disk and for a Voltalef 3S mull. As discussed above, the error limits for these distances may be underestimated in the crystallographic calculations. Beyond this, we can only attribute the single band observed to a coincidence of the bands arising from the two distinct OH groups.

Although both phosphonate **2a** and phosphine oxide **2b** have similar dimeric hydrogen bonded structures in the crystal, there is a significant difference in the position of the OH bands in the solid state (3309 cm^{-1} for **2a** and 3197 cm^{-1} for **2b**). This difference is attributed to the stronger intermolecular hydrogen bond for the phosphine oxide, as indicated by the O---O distances in the solid-state structures. However in $DCCl_3$ solutions, and in contrast to phosphonate **2a**, phosphine oxide **2b** even in highly concentrated solutions (4.3 mol %) exists mainly as intramolecular hydrogen bonded monomers, which may reflect a destabilizing effect by the comparatively bulkier phenyl groups on the dimeric structures in solution.

The IR data indicate that the intramolecular hydrogen bonding mode adopted in the crystal structure of diphenylphosphine oxide **2c** (R^1 = Bu^t) (3438 cm^{-1}) is retained in solution (3412 cm^{-1} in 0.2 mol % to 2.2 mol % $DCCl_3$ solutions and 3417 cm^{-1} in very dilute tetrachloromethane solution). In $DCCl_3$ a weak higher frequency band, which is assigned to monomers with free OH groups, appears at about 3620 cm^{-1}. The area of this band indicates that the population of such monomers is small (about 2%).

In contrast to diphenylphosphine oxide **2b**, for dimethylphosphine oxides **2d** and **2e** the intermolecular hydrogen bonded associates are more stable and are present even in dilute solutions. The single band at 3185 cm^{-1} for the intermolecular hydrogen bonded chains of solid **2d** (R^2 = Ph) is replaced in $DCCl_3$ solutions by one major broad OH band extending at its base from 3000 to 3500 cm^{-1}, which is attributed to a dimeric−monomeric equilibrium with the former predominating. Upon dilution its maximum shifts to higher wavenumbers (from 3267 cm^{-1} for 4.3 mol % solution to 3369 cm^{-1} for 0.2 mol % solution) in accordance with a shift in equilibrium from dimers toward intramolecular hydrogen bonded monomers. The mobility in solution is expected constantly to break up any polymeric structure to give dimers B in equilibrium with intramolecular hydrogen bonded monomers C as envisaged in Figure 7. This interconversion of B and C is envisioned as proceeding via a low concentration of open chain dimers (A) since it is unlikely that both hydrogen bonds will be broken or formed at the same time. It is anticipated that, unlike the case of carbonyl groups, upon ring opening of the chelate structure B there will be free rotation about the phosphoryl bond, with the hydrogen bonded molecule swinging away allowing a nonbonded lone pair of electrons to become available for the formation of an intramolecular hydrogen bond. The IR spectra in $DCCl_3$ solutions also shows the presence of a second OH band due to a small proportion (up to about 10%) of structures with non hydrogen bonded hydroxyl groups (ν_{OH}, 3608 cm^{-1}) whose concentration appears (as expected) to be proportional to the concentration of intramolecularly hydrogen bonded monomers. For more concentrated solutions, consisting mainly of dimers

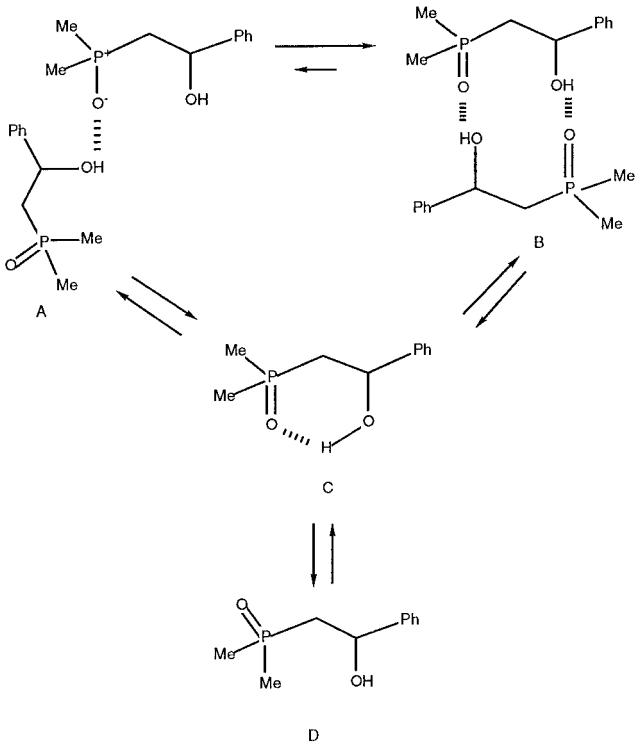

Figure 7. Process of dissociation of the polymeric chains of phosphine oxide **2d** in chloroform-*d* solutions.

B in equilibrium with monomers C, this band can be attributed primarily to the free hydroxyl groups in the open chain dimers A. In more dilute solutions with a large proportion of monomers C the non hydrogen bonded monomers D may be present. In the spectrum of highly dilute tetrachloromethane solution ($<3 \times 10^{-3}$ mol %) a band from intramolecular hydrogen bonded monomers is observed at 3379 cm^{-1}.

The IR spectra of dimethylphosphine oxide **2e** (R^2 = Bu^t) in $DCCl_3$ solutions show the same trend as phosphine oxide **2d**. Thus phosphine oxide **2e** exhibits a band from hydrogen bonded dimeric species at 3217 cm^{-1} in the solid state, at 3359 cm^{-1} for 2.2 mol % solution, and at 3398 cm^{-1} for 0.2 mol % solution. In solution the band is broad extending at its base from 3000 to 3500 cm^{-1}. The movement of its maximum to higher wavenumbers upon dilution is attributed, as above, to a changing equilibrium between intermolecularly hydrogen bonded dimers and intramolecular hydrogen bonded monomers, which shifts in favor of the monomers upon dilution.

B. Studies Based on NMR Spectroscopy. The $^3J_{HH}$ values of compounds **2a**−**e** in $DCCl_3$ strongly imply a *ga* comformer, as in the solid state. A strong preference for this conformer in less polar solvents ($DCCl_3$, C_6D_6) has been previously observed for a series of (2-hydroxyalkyl)phosphonates and attributed to the favorable anti orientation between the large $R_2^1P(O)$ and R^2 groups in conformer *ga* and a stabilizing effect of intramolecular hydrogen bonding between the phosphoryl and the hydroxyl groups.[2c]

^{1}H NMR spectra of solutions of phosphonate **2a** and phosphine oxide **2d** in $DCCl_3$ at different concentrations (0.2−4.3 mol %) and also spectra of phosphonate **2a** in tetrachloromethane solutions (0.2−2.2 mol %) were recorded in order to investigate the role of the intramolecular hydrogen bonding in determining the position of

Table 4. Chemical Shifts of the α-Methylene Protons and the Phosphorus Nucleus (ppm), Vicinal Proton−Proton and Phosphorus−Carbon Coupling Constants (Hz), and Conformer Populations for Compounds 2 (%)[a]

compd	solvent	δ_A	δ_B	$^3J_{AM}$	$^3J_{BM}$	N_{ga}	N_{ag}	N_{gg}	δ_M	$^3J_{PH}$	$^3J_{PC}$	δP
2a	CCl_4	2.02	2.11	2.9	10.4	86	7	7	5.03	9.9	15.9	31.51
	$DCCl_3$	2.18	2.26	2.8	10.2	85	5	10	5.12	10.5	15.9	31.67
	$(CD_3)_2CO$	2.17	2.22	4.1	9.5	74	20	6	5.05	9.3	14.3	31.50
	C_5D_5N	2.51	2.66	3.8	9.5	75	16	9	5.57	9.3	14.3	30.17
	$(CD_3)_2SO$	2.13	2.21	4.3	9.1	70	21	9	5.58	8.7	14.3	30.96
	CD_3OD	2.23	2.33	5.0	8.9	66	30	4	4.99	8.7	12.7	30.98
2b	$DCCl_3$	2.58	2.76	1.8	10.9	94	−6	10	5.17	9.8	13.7	34.00
	$(CD_3)_2CO$	2.87	2.70	2.5	10.3	88	1	11	5.11	9.8	12.7	32.76
	C_5D_5N	2.94	3.21	3.1	9.5	78	7	15	5.70	9.3	12.2	30.03
	$(CD_3)_2SO$	2.72	2.95	4.0	9.0	71	17	12	5.51	8.7	10.8	29.26
	CD_3OD	2.75	2.95	4.8	8.5	64	26	10	5.13	8.6	9.8	34.25
2c	$DCCl_3$	2.42	2.33	1.2	11.1	97	−12	15	3.69	10.5	12.2	36.18
	$(CD_3)_2CO$	2.80	2.29	1.2	11.0	96	−12	16	3.59	10.9	12.2	35.55
	C_5D_5N	2.72	2.62	1.2	11.1	97	−12	15	4.02	10.5	11.7	33.56
	$(CD_3)_2SO$	2.58	2.37	1.0	10.7	93	−15	22	3.56	10.6	11.7	33.15
	CD_3OD	2.56	2.50	1.4	11.2	97	−9	12	3.70	11.7	11.7	37.69
2d	$DCCl_3$	2.07	2.21	2.7	10.4	88	4	8	5.27	10.0	11.3	44.68
	C_5D_5N	2.31	2.43	2.9	10.1	84	6	10	5.67	9.5	11.7	40.70
	$(CD_3)_2SO$	2.03	2.10	3.4	9.8	79	12	9	4.98	9.0	11.3	41.32
	CD_3OD	2.16	2.28	3.6	9.4	75	14	11	5.08	9.0	10.8	49.11
2e	$DCCl_3$	1.86	1.82	1.5	11.3	96	−8	11	3.80	9.6	11.3	46.32
	$(CD_3)_2CO$	1.90	1.78	1.6	11.3	96	−6	10	3.74	10.0	11.7	46.60
	C_5D_5N	2.07	1.99	1.6	11.0	94	−7	13	4.10	10.3	11.3	43.40
	$(CD_3)_2SO$	1.82	1.63	1.0	11.0	95	−14	19	3.54	10.9	11.3	44.33
	CD_3OD	2.00	1.82	1.3	11.2	95	−9	14	3.66	10.8	11.3	51.40

[a] The spectra are of 2.2 mol % solutions.

the conformational equilibrium. IR spectral analysis indicated that the changes in the nature of the hydrogen bonding in these solutions do not influence the relative populations of conformers *ga*, *ag*, and *gg* appreciably. However, our recent structural study of (2-hydroxypentyl)diphenylphosphine oxide (**2f**) showed that the change of the nature of the bonding from intermolecular in the crystal to intramolecular in less polar solvents, such as $DCCl_3$ and C_6D_6, leads to different conformational preferences in the solid state and in solution.[7] Thus, in the case of large substituent R^2 (Ph, Bu^t), its bulk governs the conformational preferences, whereas as the size of R^2 decreases, the nature of the hydrogen bonding plays an increasingly important part in determining the position of the conformational equilibrium.

Conformational Preferences in Polar Solvents. The NMR spectra of phosphonate **2a** and phosphine oxides **2b** and **2c** (R^2 = Ph) in more polar solvents, such as DMSO-d_6 and methanol-d_4, indicate a decrease in the population of conformer *ga*, while the population of conformer *ag* increases relative to that in $DCCl_3$ solution (Table 4). For example, the population of conformer *ga* for **2b** is estimated to be 90% in $DCCl_3$, but decreases to 64% in methanol-d_4. The values of the torsion angle dependent vicinal phosphorus−carbon couplings ($^3J_{PC}$)[12] support this trend, e.g. $^3J_{PC}$ for phosphine oxide **2b** in $DCCl_3$ is 13.7 Hz, and 9.8 Hz in methanol-d_4 solution. The influence of the polar solvents on the conformational distribution is attributed to the solvation of the phosphoryl and the hydroxyl groups and the formation of solvent−solute associates. However, despite this polar solvent effect, *ga* remains the favored conformer.

For phosphine oxides **2c** and **2e** (R^2 = Bu^t) negative values for the population of conformer *ag* were obtained from calculations based on perfectly staggered geometries which, in addition, gave surprisingly high contributions of conformer *gg* despite the unfavorable gauche orientation between the bulky groups. However, the experimental vicinal proton−proton and phosphorus−carbon coupling constants for phosphine oxides **2c** and **2e** show very little solvent dependence (Table 4). The consistently high values of $^3J_{PC}$ are indicative of anti relationship between the phosphoryl and the tertiary butyl groups, i.e., preference for conformer *ga*. The values of both $^3J_{AM}$ and $^3J_{BM}$ (Table 4) are less than the calculated coupling constants for the perfectly staggered conformer *ga* (the calculated values of $^3J_{AM}(ga)$ and $^3J_{BM}(ga)$ for phosphine oxide **2c** are 2.0 and 11.7 Hz, respectively; the corresponding values for phosphine oxide **2e** are 2.0 and 11.8 Hz). It is been previously demonstrated that the tertiary butyl group can block any rotation around a specific bond in acyclic sulfur compounds and can also induce significant torsion angle deformations.[13] MM modeling studies of **2c** and **2e** not only indicated strong preference for conformer *ga* but also predicted distortion from the perfectly staggered form. The values of $^3J_g(ga)$ and $^3J_a(ga)$ calculated with the MM predicted torsional angles H^AC1C2H^M and H^BC1C2H^M in the vapor phase (70.5° and −168.5° for **2c** and 68.2° and −171.9° for **2e**) were 1.1 and 10.8 Hz for **2c** and 1.2 and 11.2 Hz for **2e**, respectively. These values are much closer to the values of the observed couplings compared to the values of $^3J_g(ga)$ and $^3J_a(ga)$ obtained using 60° and 180°. Therefore it is concluded that while the tertiary butyl group hinders rotation around the C1−C2 bond of phosphine oxides **2c** and **2e**, there is sufficient mobility about this bond to produce an average twisted version of conformer *ga* (Figure 8). The population of only one conformer allows the estimation[14] of the average degree of distortion from the perfectly staggered geometry to be between 4° and 12° (Table 5) depending on the solvent.

(12) Quin, L. D. In *Methods in Stereochemical Analysis*; Marchand, A. P., Series Ed.; VCH Publishers: New York, 1987; Vol. 8, Chapter 12.

(13) Fernandez, I.; Liera, J. M.; Zorrilla, F.; Alcudia, F. *Tetrahedron* **1989**, *45*, 2703−2718.

(14) Haasnoot, C. A. G.; de Leeuw, F. A. A. M.; Altona, C. *Tetrahedron* **1980**, *36*, 2783−2792.

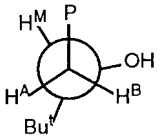

Figure 8. Distorted conformer *ga* adopted by phosphine oxides **2c** and **2e** in solution.

Table 5. Values of Dihedral Angles H^AC1C2H^M and H^BC1C2H^M (deg) for 2c and 2e, Calculated by the Haasnoot−Altona Equation (and from the crystal structures)

compd	solvent	H^AC1C2H^M	H^BC1C2H^M
2c	$CDCl_3$	69	188
	$(CD_3)_2CO$	70	190
	C_5D_5N	69	188
	$(CD_3)_2SO$	72	192
	CD_3OD	66	188
	(x-ray)	71	190
2e	$CDCl_3$	65	187
	$(CD_3)_2CO$	64	187
	C_5D_5N	64	190
	$(CD_3)_2SO$	71	190
	CD_3OD	68	189
	(x-ray)	70	187

The values of the vicinal phosphorus−proton coupling constants ($^3J_{PH}$), which are also torsion angle dependent,[15] vary between 8.6 and 11.7 Hz, in accordance with a gauche relationship between the phosphorus and proton nuclei. However, their usefulness in this study is limited by the fact that the phosphorus and proton nuclei are gauche in the conformers whose populations are varying most (*ga* and *ag*), and thus the coupling is little affected by changes in the relative populations of these conformers. In addition, the substituent and the solvent effects on this coupling constant have been little studied.

Molecular Modeling Studies. For compounds **2a**−**e** molecular mechanics (MM) modeling of conformers *ga*, *ag*, and *gg* predicted, as expected, that in the vapor phase, conformers *ga* and *gg* are between 2.8 and 5.0 kcal mol^{-1} more stable when an intramolecular hydrogen bond is formed. For phosphonate **2a**, MM modeling indicated that the intramolecular hydrogen bonding can involve either the phosphoryl oxygen or a phosphonic ester oxygen, with the latter being favored. To examine the possibility for the formation of such an unusual bond, ab initio studies on phosphonate **2a** were carried out. In contrast to MM modeling, optimization of the molecular geometry of **2a** at the HF/6-31G*//HF/3-21G$^{(*)}$ level[16] showed that the intramolecular hydrogen bonding to the phosphoryl oxygen is preferred by 2.3 kcal mol^{-1} for conformer *ga* and by 5.0 kcal mol^{-1} for conformer *gg*. Both MM and ab initio calculations gave O---H separations of ~1.9 Å which is in agreement with the value of 1.92(3) Å determined for intramolecular hydrogen bonded phosphine oxide **1c** by X-ray crystallography.[3b] We conclude that the prediction by MM modeling of a hydrogen bond to a phosphonic ester oxygen being more stable comes from erroneous charge calculations, which give the phosphonic ester oxygen a larger negative charge than the phosphoryl oxygen. In addition we have no experimental evidence for the formation of such a bond, observing instead that the crystal structure of **2a** consists of dimers, involving hydrogen bonding to the phosphoryl oxygen. Furthermore, the NMR and IR spectra of **2a** show the same trends, for example on dilution, as those of phosphine oxides **2b**−**d**, where hydrogen bonding is only possible to the phosphoryl oxygen.

As previously observed for phosphine oxide **2f**,[7] MM modeling of the vapor phase stereochemistry of phosphonate **2a** and phosphine oxides **2b** and **2d** (R^2 = Ph) predicted intramolecular hydrogen bonded conformer *gg* to be the most stable. As before, intramolecular van der Waals (VDW) interactions were a key factor contributing to this preference. Thus for **2d** the VDW interactions stabilized conformer *gg* relative to the intramolecular hydrogen bonded conformer *ga* by 1.2 kcal mol^{-1}. MM simulation of the solvation of **2a**, **2b**, and **2d** off-set the intramolecular VDW effect. Although such modeling covers only the initial stages of solvation, it should reveal the most important solvent−solute interactions since it has been reported that docking of five or six solvent molecules was sufficient to complete the first solvation shell of a pyridinium betaine.[17] Thus, after docking of five molecules of either chloroform, acetone, pyridine, or methanol with conformers *ga*, *ag*, or *gg*, conformer *ga* became the most favored in each case, which is in accordance with the results from the NMR study. The ab initio study on phosphonate **2a** at the HF/3-21G$^{(*)}$[16] level also predicted conformer *gg* as the most stable in the vapor phase. However, calculations at the HF/6-31G*//HF/3-21G$^{(*)}$ level showed conformer *ga* as being by 0.6 kcal mol^{-1} more stable than conformer *gg* and by 2.9 kcal mol^{-1} more stable than conformer *ag*. In the latter calculations the partial charges were of a lower magnitude and it seems probable that Coulombic energies were responsible for the energy differences. Conformers *ga*, *ag*, and *gg* calculated for phosphonate **2a** at the HF/6-31G*//HF/3-21G$^{(*)}$ level are presented in Figure 9. Selected structural parameters are given in Table 6.

For phosphine oxides **2c** and **2e** (R^2 = Bu^t) conformer *ga* was predicted as most stable in both the vapor phase and when solvated. MM modeling indicated that the polar solvents stabilize non hydrogen bonded conformers through intermolecular hydrogen bonding to the hydroxyl group (acetone, pyridine, methanol) and the phosphoryl group (methanol). In the case of methanol for all compounds, conformers *ga* and *gg* were shown to be more stable when the phosphoryl and the hydroxyl group are not intramolecularly hydrogen bonded but are involved in intermolecular hydrogen bonding with the solvent molecules.

NMR Chemical Shifts of the α-Methylene Protons H^A and H^B. The α-methylene protons H^A and H^B are diastereotopic and therefore anisochronous. The chemical shift difference of these protons is strongly dependent on the nature of the substituents R^1 and R^2 and the solvent (Table 4). When R^2 is tertiary butyl (phosphine oxides **2c** and **2e**), the signal of H^A always appears downfield of H^B. On the other hand when R^2 is phenyl (phosphonate **2a** and phosphine oxides **2b** and **2d**) the signal of H^A is observed at higher field. Since in $DCCl_3$ the compounds have similar preferences for conformer *ga* (see above), the difference in the chemical shifts of

(15) Bentrude, W. G.; Setzer, W. N. In *Methods in Stereochemical Analysis*; Marchand, A. P., Series Ed.; VCH Publishers: New York, 1987; Vol. 8, Chapter 11.

(16) Hehre, W. J.; Radom, L.; Schleyer, P.v. R.; Pople, J. A. In *Ab Initio Molecular Orbital Theory*; Wiley: New York, 1986; Chapter 6.

(17) Beckett, M. A.; Dawber, J. G. *J. Chem. Soc., Faraday Trans. 1* **1989**, *85*, 727−733.

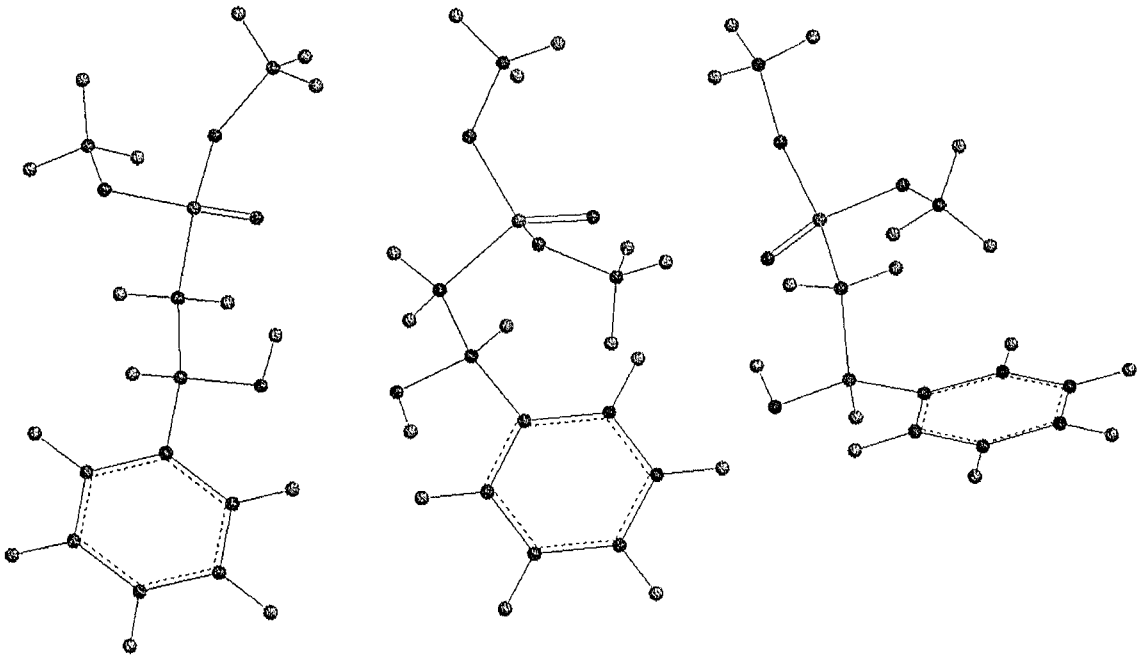

Figure 9. Conformers *ga*, *ag*, and *gg* of phosphonate **2a** at HF/6-31G*//HF/3-21G(*).

Table 6. Selected Structural Parameters for Conformers *ga*, *ag*, and *gg* for Phosphonate 2a Calculated at the HF/6-31G*//HF/3-21G(*) Level[a]

	ga	*ag*	*gg*
	Bond Lengths (Å)		
P−O1	1.475	1.468	1.474
P−O3	1.574	1.577	1.574
P−O4	1.578	1.581	1.573
P−C1	1.777	1.785	1.784
C1−C2	1.559	1.538	1.558
C2−C3	1.513	1.523	1.519
C2−O2	1.432	1.445	1.432
O1---O2 (O1---H2O2)	2.773 (1.918)	4.428 (4.945)	2.734 (1.861)
	Bond Angles (deg)		
O1−P−C1	114.47	115.25	112.95
O1−P−O3	113.08	115.67	112.62
O1−P−O4	112.44	112.79	115.72
O3−P−C1	105.58	101.61	109.00
O4−P−C1	103.44	107.66	102.33
O3−P−O4	107.03	102.49	103.23
P−C1−C2	110.62	113.43	112.12
C1−C2−C3	109.39	112.85	112.25
C1−C2−O2	109.97	103.98	110.68
O2−C2−C3	108.33	110.69	111.79
	Torsion Angles (deg)		
P−C1−C2−O2	62.34	168.66	−59.02
P−C1−C2−C3	−178.80	−71.34	66.65
O1−P−C1−C2	−39.15	−20.15	33.65
H^A−C1−C2−H^M	63.25	174.88	−56.07
H^B−C1−C2−H^M	−178.83	−68.76	61.65
dipole moment (*D*)	4.334678	2.377658	4.573545

[a] The numbering scheme from the X-ray structure of 2a has been used.

the α-methylene protons appears to be related to the different shielding properties of the tertiary butyl and the phenyl groups. An examination of the *ab initio* optimized conformer *ga* of phosphonate **2a** indicated that H^A is closer to the plane of the phenyl ring than H^B. Such orientation would situate H^A in the shielding region of the aromatic system and explain the observed upfield shift.

The spectra of acetone-d_6 solutions of phosphine oxides **2b** and **2c** (R^1 = Ph) revealed an unexpected effect of this solvent on the chemical shifts of the α-methylene protons. For **2b** in acetone-d_6, H^A is observed at lower field than H^B which is in contrast to the other solvents. In the case of **2c**, acetone-d_6 induces an exceptionally large chemical shift difference between H^A and H^B (Δ_{AB} = 0.52 ppm). In contrast to phosphine oxides **2b** and **2c** (R^1 = Ph), phosphonate **2a** (R^1 = MeO), and phosphine oxide **2e** (R^1 = Me) do not experience a similar acetone-d_6 effect. Thus the chemical shifts of H^A and H^B in acetone-d_6 are not very different from those in $DCCl_3$. It seems less likely that this is due to a difference in the acidity of the α-methylene protons since the acidity of the α-methylene protons of phosphine oxide **2e** and phosphonate **2a** would be expected to be lower and higher, respectively, compared to **2b** and **2c**. It is well-known that polarized C−H groups may form weak hydrogen bonds with oxygen acceptors and the general structural properties of these interactions and their relation to conventional hydrogen bonds such as O−H---O have recently been reviewed.[18] It is also noted that acetone does not compete with the phosphoryl group for hydrogen bonding to the hydroxyl proton in accordance with phosphine oxides being stronger bases than carbonyl compounds.[19] Therefore it was of interest to investigate the chemical shift difference of H^A and H^B for **2c** across of range of chloroform−acetone mixtures. This showed (see Figure 10) that the exceptionally large difference is due to the marked downfield shift of the H^A signal in acetone-d_6. The effect is attributed to weak hydrogen bonding between the carbonyl oxygen of acetone-d_6 and H^A in combination with the *P*-phenyl groups adopting a stereochemistry which favors a specific orientation of acetone-d_6 toward H^A. This explanation is supported by the linear change of δ_A with

(18) Steiner, T. *Chem. Commun.* **1997**, 727−734.
(19) Edmundson, R. S. In *The Chemistry of Organophosphorus Compounds*; Hartley, F. R., Ed.; Wiley & Sons Ltd.: New York, 1992; Vol. 2, Chapter 7.

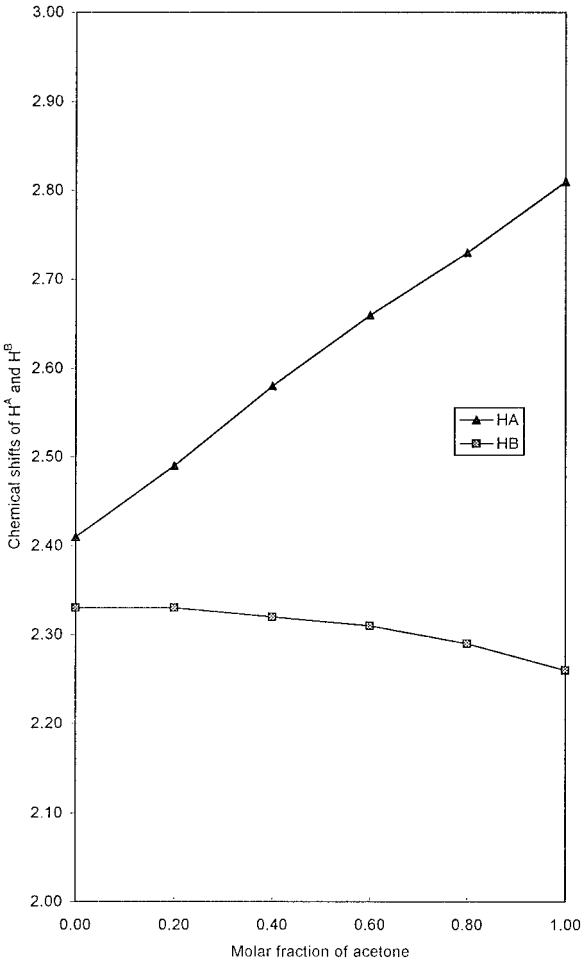

Figure 10. Chemical shifts of H^A and H^B for phosphine oxide **2c** in chloroform−acetone mixtures.

the molar fraction of acetone-d_6 (see Figure 10) which indicates that the lifetime of the solvent−solute associates is not affected by solvent composition. From the small shift of H^B in the opposite direction it is possible that electrostatic repulsion between acetone and the hydroxyl oxygen disfavors a specific orientation of the solvent molecules toward H^B.

Pyridine-d_5 produces downfield shifts of both H^A and H^B relative to $DCCl_3$ for all compounds. For phosphine oxides **2c** and **2e**, in which the conformational preference is the same in both solvents, the deshielding of H^A and H^B is of similar magnitude. MM modeling studies of the solvation of compounds **2a**−**e** by pyridine indicated that the nitrogen atom of the solvent molecule can associate not only with the hydroxyl hydrogen, but also with other electropositive sites in the solute molecule such as H^A, H^B, or H^M. In the intramolecular hydrogen bonded conformer *ga*, the pyridine molecules could associate with H^A with a preferred orientation in the same manner as acetone, which would account for the downfield shift of this proton. However, unlike the solvation effects of acetone, H^B is also deshielded. This could be attributed to the greater basicity of the pyridine molecule which competes with the phosphoryl oxygen for hydrogen bonding to the hydroxyl group. This would set up an equilibrium between solute molecules adopting conformer *ga* with an intramolecular hydrogen bond and molecules adopting the same conformer but with intermolecular hydrogen bonding to pyridine molecules. NMR study of cyclic hydroxylic compounds has shown that the formation of hydrogen bonding in pyridine solutions induces lower field shifts of the protons, occupying vicinal position to the hydroxyl group.[20] The extent of deshielding is dependent upon the torsion angle between the proton and the hydroxyl group, being larger when the torsion angle is smaller.[20] Thus such an effect can also explain the downfield shifts of H^B, which has a gauche relationship with the OH group in conformer *ga*.

^{31}P Chemical Shifts. The ^{31}P NMR chemical shifts exhibit marked dependence on the nature of the solvent (Table 4). For **2b**−**e** downfield shifts of the ^{31}P signals are observed in methanol-d_4 relative to the other solvents, the effect being several ppm greater for the dimethylphosphine oxides compared to the diphenylphosphine oxides in accordance with the greater inductive electron-donating properties of the methyl groups. This deshielding can be attributed to solvent providing additional hydrogen bonding to the phosphoryl oxygen, which enhances σ-bond polarization and modifies π back-bonding to phosphorus. $DCCl_3$ also causes downfield shifts, which can be explained by preferential solvation of the type P═O---$HCCl_3$. The formation of such solvent−solute associates was also predicted by MM modeling. In solvents without hydrogen-donating properties, e.g. DMSO-d_6, the ^{31}P signals occurred at higher field.

Conclusion

The intermolecular hydrogen bonding via the formation of inversion-center-related cyclic dimers and to a lesser extent intermolecular polymeric chains emerges as a common solid state arrangement.[21] Polymeric hydrogen bonded chains in the solid state dissociate on dissolution into an equilibrium mixture of dimers and monomers. Solid state hydrogen bonded dimers usually produce a dimer−monomer equilibrium in solution which can become extensively shifted in favor of intramolecular hydrogen bonded monomers when bulky groups (R^1 and R^2) are present. When intermolecular hydrogen bonding is sufficiently destabilized by bulky groups (e.g. **2c**), intramolecular hydrogen bonded monomers are adopted both in the solid and across a wide range of solution concentrations. The nature of the hydrogen bonding has little influence on the conformational preference of compounds with large R^2 (Bu^t, Ph etc.); however, solvation by a polar solvent can destabilize the favored conformer *ga*. The extent to which mobility in solution distorts the staggered conformer *ga* has been estimated to be 4−12° depending on the solvent.

Experimental Section

General Considerations. ^{1}H and ^{13}C NMR spectra of **2a**−**e** were recorded on a JEOL GSX-270 spectrometer or on a JEOL JNM-FX270 spectrometer. All ^{1}H and ^{13}C NMR measurements were referenced to internal Me_4Si. ^{31}P NMR spectra were recorded on a JEOL GSX-270 spectrometer or a JEOL FX90Q spectrometer and referenced to external 85% H_3PO_4. The vicinal proton−proton coupling constants $^3J_{AM}$ and $^3J_{BM}$ and the chemical shifts of the α-methylene protons H^A and H^B were obtained by spectroscopic analysis of the signal from these protons, representing an AB part of an ABMX spin system. The analyses were carried out using the

(20) Demarco, P. V.; Farkas, E.; Doddrell, D.; Mylari, B. L.; Wekert, E. *J. Am. Chem. Soc.* **1968**, *90*, 5480−5486.

LAOCOON IV program.[22] The parameters were accurate to 0.1 Hz or better. The conformational preferences were evaluated by means of NMR spectroscopy relating the observed vicinal proton−proton coupling constants to the couplings in the individual conformers:

$$J_{obs} = \sum_{i=1,3} n_i J_i$$

$$n_1 + n_2 + n_3 = 1$$

The proton−proton coupling constants in the individual conformers were calculated using the Haasnoot−Altona equation[14] and the group electronegativities reported by Inamoto et al.[23] Full details about the spectral analysis and the assignment of the diastereotopic α-methylene protons H^A and H^B are given in ref 2c.

IR spectra of **2a**−**e** in solid state (KBr disks) and in $DCCl_3$ and tetrachloromethane solutions were recorded on a Nicolet Impact 400 spectrometer. The solution concentrations are given in mol % in order to have the same molar ratio between solvent and solute in all cases. For the solutions, sodium chloride cells with 0.5 mm path length and quartz cells with 5 cm path length were used. The solvents were obtained commercially and used without further purification.

Determination of molecular weight for phosphonate **2a** was carried out as previously described.[11]

Computer Simulations. MM modeling was carried out using the COSMIC-90 program.[24] Partial charges were calculated by the LIVERPOOL-2 method.[25]

The calculations were carried out using bond lengths (P═O, P−C, P−O) and bond angles (OPC, CPC, OPO, PCC, etc.) obtained from our X-ray crystallographic studies. The reason for this was that the P═O bond length included in the original COSMIC force field is 1.428 Å, whereas it has been reported that the P═O length is usually in the range of 1.475−1.490 Å and it is almost insensitive to molecular environment, hydrogen bonding, or the nature of any substituents.[26] Similarly, bond angles involving phosphorus are not included in the force field, and a default value of 109.5° is normally used; X-ray data for phosphine oxides have shown that there is a consistent deviation of the bond angles from the tetrahedral values with CPO higher (112−114°) and CPC lower (104−107°).[26]

Each structure was then optimized by well-established methods such as CONJUGATE GRADIENT and TORMIN. The different conformers, produced upon rotation of all rotatable bonds in 5° steps, were further minimized and stored.

In the molecular-docking program the stationary molecule, in this case one of the conformers *ga*, *ag*, and *gg*, is placed at the center of 1 nm diameter sphere, and the mobile molecule (the single solvent molecule) is placed in turn at points on the sphere, in all a total of 204 of such starting points. At each starting point the mobile molecule is rotated about its axis in 60° steps about all three Cartesian axes, and the lowest energy obtained is used as the starting orientation for a subsequent energy-minimization procedure involving 500 iterations or until the change in energy between succesive iterations is <0.0001 kcal mol^{-1}. In this procedure the bimolecular species of lowest energy from the first docking process was stored, further minimized, and used in the next run as the fixed species. For each compound, multiple dockings with either five molecules of $CHCl_3$ or C_5H_5N or $(CH_3)_2CO$ or CH_3OH to each of conformers *ga*, *ag*, or *gg*.

The ab initio calculations were carried out using SPARTAN SGI Version 4.1.2[27] on a SGI O_2 180 MHz R5000SC 64Mb RAM IRIX 6.3 computer. A list of 27 conformers was generated with the SYBYL MM force field[28] by rotation about the C1−C2, P−C1, and C2−O2 bonds. All conformers were further optimized using the PM3 method.[29] Then the most stable conformers were optimized at the HF/3-21G(*) level.[16] Single-point calculations were performed with the HF method using a 6-31G* basis set.[16]

X-ray Crystal Structure Determinations. Procedure. Data were recorded on a FAST TV detector diffractometer (Mo Kα radiation) using previously described methods[30] and corrected for Lorentz and polarization effects. Systematically absent data indicated the space group in each case. Most non-H atom positions were estimated using direct methods,[31] and all were located by means of sequential difference Fourier syntheses.[32] These atoms were refined[32] anisotropically using merged data. Hydrogen atoms were introduced in theoretical positions (OH, 0.82; $C_{aryl}H$, 0.93; $C_{methine}H$, 0.98; $C_{methylene}H$, 0.97; $C_{methyl}H$, 0.96 Å) and assigned common, refined, isotropic displacement parameters according to three types, namely aromatic, methyl, and aliphatic nonmethyl. Finally, an absorption correction[33] based on these converged models was applied to the data and degrees of freedom restricted appropriately for the final refinement[32] cycles. The weighting scheme was $w^{-1} = \sigma^2(F_o)^2 + xP^2$, where $3P = (F_o)^2 + 2(F_c)^2$ (Table 1). A listing of specific details is given in Table 1.

Synthesis. The synthesis of phosphonate **2a** is described elsewhere.[2c]

General Procedure for Preparation of (2-Hydroxyalkyl)diphenylphosphine Oxides.[5] To a stirred solution of diphenylmethylphosphine oxide in dry THF was added a solution of 1.6 M *n*-butyllithium at 0 °C under N_2. After 30 min, the reaction solution was cooled to −78 °C (acetone−solid CO_2), and a solution of appropriate aldehyde in THF was added dropwise at such a rate that the solution temperature was maintained at −78 °C. The reaction mixture was allowed to warm to room temperature over 2 h, and water was added. THF was removed under reduced pressure, and brine was added to the aqueous residue before extraction with dichloromethane. The extract was dried ($MgSO_4$), and dichloromethane was evaporated to give the crude product. In this way the following compounds were prepared.

(2-Hydroxy-2-phenylethyl)diphenylphosphine Oxide (2b). Diphenylmethylphosphine oxide (4 g, 18.6 mmol), *n*-BuLi (1.6 M in hexane, 12.5 mL, 18.6 mmol), and benzaldehyde (2.1 g, 20.4 mmol) were reacted as above to produce a viscous oil, which after washing with hexane crystallized. It was purified by recrystallization from hexane/acetone to give white crystals (4.8 g, 80%): mp 143−145 °C; IR (KBr)/cm^{-1} 3197 (OH), 1179 (P═O). Anal. Calcd for $C_{20}H_{19}O_2P$: C, 74.52; H, 5.94. Found: C, 74.78; H, 6.00%.

(2-Hydroxy-3,3-dimethylbutyl)diphenylphosphine Oxide (2c). Diphenylmethylphosphine oxide (2 g, 9.3 mmol), *n*-BuLi (1.6 M in hexane, 6.3 mL, 9.6 mmol), and trimethylacetaldehyde (0.88 g, 10.2 mmol) reacted as above giving a crystalline product, which was purified by recrystallization

(21) A good overview of phosphoryl infrared spectroscopy can be found in Thomas, L. C. *Interpretation of the Infrared Spectra of Organophosphorus Compounds*; Heyden: New York, 1994.

(22) Castellano, S. M.; A. A. Bothner-By, *J. Chem. Phys.* **1967**, *47*, 5443.

(23) Inamoto, N.; Masuda, S. *Chem. Lett.* **1982**, 1003−1006.

(24) (a) Vinter, J. G.; Davies, A.; Saunders: M. R *J. Comput.-Aided Mol. Des.* **1987**, *1*, 31−51. (b) Moley, S. D.; Abraham, R. J.; Hawarth, I. S., Jackson, D. E.; Saunders: M. R.; Vinter, J. G. *J. Comput.-Aided Mol. Des.* **1991**, *5*, 475−504.

(25) (a) Abraham, R. J.; Griffiths, L.; Loftus, P. J. *J. Comput. Chem.* **1982**, *3*, 407−416. (b) Abraham, R. J.; Hudson, B. D. *J. Comput. Chem.* **1984**, *5*, 562−570. (c) Abraham, R. J.; Hudson, B. D. *J. Comput. Chem.* **1985**, *6*, 173−181.

(26) Gilheany, D. In *The Chemistry of Organophosphorus Compounds*; Hartley, F., Ed., Wiley & Sons Ltd.: New York, 1992; Vol. 2, Chapter 1.

(27) SPARTAN Version 4.1.2. SGI IRIX 6.3.; Wavefunction, Inc., 18401 Von Karman Ave., no. 370, Irvine, CA 92715.

(28) Clark, M.; Cramer III, R. D.; Opdensch, N. *J. Comput. Chem.* **1989**, *10*, 982−1012.

(29) Stewart, J. J. P. *J. Comput. Chem.* **1989**, *10*, 209−220.

(30) Darr, J. A.; Drake, S. R.; Hursthouse, M. B.; Malik, K. M. A. *Inorg. Chem.*, **1993**, *32*, 5704−5708.

(31) Sheldrick, G. M. *SHELXS-86, Program for the Solution of Crystal Structures*, University of Goettingen, 1987.

(32) Sheldrick, G. M. *SHELXL-93, Program for the Refinement of Crystal Structures*, University of Goettingen, 1993.

(33) Walker, N.; Stewart, D. *Acta Crystallogr.* **1983**, *A39*, 158−166.

(34) Davies, E. K. *SNOOPI*, Chemical Crystallography Laboratory, University of Oxford, 1982.

from hexane/acetone to give white crystals (2 g, 72%): mp 134−136 °C; IR (KBr)/cm^{-1} 3438 (OH), 1172, 1149 (P═O). Anal. Calcd for $C_{18}H_{23}O_2P$: C, 71.51;H, 7.67. Found: C, 71.35; H, 7.67%.

General Procedure for Preparation of (2-Hydroxyalkyl)dimethylphosphine Oxides.[6] Freshly distilled phosphorous acid diethyl ester {$(EtO)_2P(O)H$} was added to a solution of methylmagnesium chloride in THF at such a rate that with ice-cooling the temperature was maintained at 20−30 °C. After stirring at room temperature for 1 h, the appropriate epoxide was added, and the mixure was refluxed for 2 h. After hydrolysis with ice-cold aqueous potassium carbonate, the mixture was filtered, and the magnesium carbonate was washed with ethanol. The aqueous ethanol filtrate was evaporated under reduced pressure. The residue was dissolved in chloroform, and the solution was dried ($MgSO_4$). After the removal of the solvent, the crude product was obtained. In this way the following compounds were prepared.

(2-Hydroxy-2-phenylethyl)dimethylphosphine Oxide (2d). Phosphorous acid diethyl ester (5.2 g, 0.038 mol), methylmagnesium chloride (3 M in THF, 40 mL), and styrene oxide (5.4 g, 0.045 mol) reacted as above to give an oil which crystallized after washing with hexane. It was twice recrystallized from hexane/acetone to give white crystals (4.6 g, 61%): mp 117−119 °C; IR (KBr)/cm^{-1} 3185 (OH), 1146 (P═O). Anal. Calcd for $C_{10}H_{15}O_2P$: C, 60.60; H, 7.63. Found: C, 60.37; H, 7.80.

(2-Hydroxy-3,3-dimethylbutyl)dimethylphosphine Oxide (2e). Phosphorous acid diethyl ester (5.5 g, 0.04 mol), methylmagnesium chloride (3 M in THF, 40 mL), and 1,2-epoxy-3,3-dimethylbutane (4.5 g, 0.045 mol) reacted as above to produce a solid product, which was twice recrystallized from hexane/benzene to give white crystals (5.1 g, 72%): mp 109−112 °C; IR (KBr)/ cm^{-1} 3220 (OH), 1173, 1156 (P═O). Anal. Calcd for $C_8H_{19}O_2P$: C, 53.92; H, 10.75. Found: C, 53.99; H, 10.83.

Acknowledgment. The authors thank the Chemistry Department of Keele University for allowing use of their JEOL GSX-270 NMR spectrometer and particularly to Mr. Graham Evans for recording the spectra. We are also grateful to Mr. Steven Withington from Ceram Research for the IR spectra on the Nicolet Impact 400 spectrometer. Grateful acknowledgment is made of the use of the EPSRC X-ray Crystallography Service, Cardiff, for the collection of diffraction data. Dr. Larry Falvello and Prof. Jack Dunitz are thanked for helpful discussions.

Supporting Information Available: X-ray data (atomic coordinates, selected bond distances and angles, selected torsion angles, and structure factors) for **2a**−**e** (42 pages). This material is contained in libraries on microfiche, immediately follows this article in the microfilm version of the journal, and can be ordered from the ACS; see any current masthead page for ordering information.

JO972036O